

No Evidence for Coherent Diffractive Radiation Patterns in the Millisecond Pulsar PSR J0437–4715

M. Vivekanand

*National Center for Radio Astrophysics, TIFR,
Pune University Campus, P. O. Box 3, Ganeshkhind, Pune 411007, India. (vivek@ncra.tifr.res.in)*

arXiv:astro-ph/0105471v1 28 May 2001

ABSTRACT

An independent analysis of the 326.5 MHz data obtained by Ooty Radio Telescope reveals no evidence for coherent diffractive radiation patterns in the millisecond pulsar PSR J0437–4715.

Key words: pulsars – PSR J0437–4715 – single pulses – radio – radiation mechanism.

1 INTRODUCTION

Ables et al (1997) (henceforth AMDV) claimed that they observed periodic variation in the distribution of the positions (or phases) of the spiky emission in the millisecond pulsar PSR J0437–4715. Their data were obtained at 326.5 MHz with the Ooty Radio Telescope (ORT) using the incoherent de-dispersion technique; only a single linear polarization was available. The sampling interval of their data was 102.4 micro seconds (μ s), but they apparently discovered a much smaller period of $\approx 20 \mu$ s for the fringes in the distribution of positions of spikes. They state they could do so because “in these distributions there is almost no noise in the traditional sense”, so they assumed the typical rms error on the positions of the spikes to be about 1.7μ s (“Gaussian of 4μ s FWHM”); this is much smaller than either the sampling interval or the fringe period. They state that the above was evidence for “diffraction fringes associated with coherent emission from a finite aperture” on the pulsar.

This was refuted by Jenet et al (1998), who analyzed PSR J0437–4715 data obtained at 1380 MHz with the Parkes Observatory. Using the coherent de-dispersion technique, they obtained a time resolution of 0.32μ s, which is much shorter than even the expected $\approx 4.7 \mu$ s fringe spacing at 1380 MHz, if the fringes are due to diffractive coherent radiation as claimed by AMDV.

This paper reports the result of an independent analysis on the data of AMDV. No evidence is found for the fringes reported by them. The possible reasons for their result are discussed.

2 OBSERVATIONS AND DATA REDUCTION

The instrument, the method of observation, and the several variations of data reduction for diverse purposes are given in AMDV, Vivekanand et al (1998) and Vivekanand (2000).

The top panel of fig. 1 shows six periods centered around

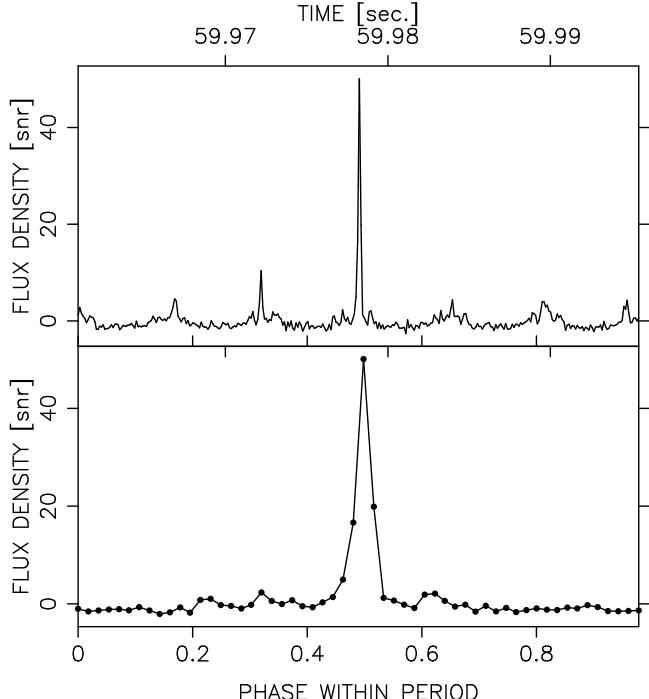


Figure 1. Similar to Fig. 1 of AMDV. **Top panel:** Six periods of data centered on the strongest spike observed in PSR J0437–4715 at 326.5 MHz using ORT (file labeled 50681546). The abscissa is in seconds measured from the start of the data file, while the ordinate is in units of the signal to noise ratio. **Bottom panel:** The period containing the spike; the abscissa is in units of the period (this is also known as phase or longitude within the period).

the highest spike in the data file labelled 50681546, observed at UT 15:46:18 on 9 Mar 1995, with a sampling interval of 102.4μ s. This file contains one of the highest sensitivity data available. The ordinate was obtained in units of the signal to noise ratio (snr) in the following manner:

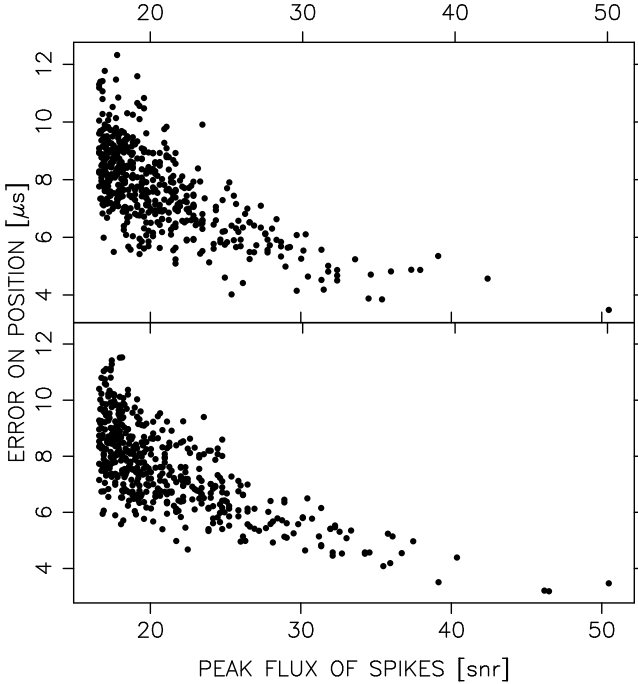


Figure 2. The height of 500 spikes (in units of signal to noise ratio) plotted against the estimated root mean square error on their positions (in micro seconds). The top panel is for data file 50681546 while the bottom panel is for data file 50681549. The expected anti-correlation is clearly visible.

First, the 681 984 continuous time samples of pulsar flux data in the file were loaded into an array of length 1 048 576, and an FFT was performed to obtain the power spectrum. The most prominent features were the pulsar fundamental at 173.688427 Hz and 27 of its harmonics. Next were the second, fourth and sixth harmonics of the power line frequency of ≈ 48 Hz (this number varies by ± 1 Hz at ORT depending upon the day and time of observation). At each of these 28 $+ 3 = 31$ spectral features, a width of 1.0 Hz was filtered out. The rest, barring a few small spikes, looked like the spectrum of random noise, and was assumed to be due to receiver noise, intrinsic pulse to pulse flux variations of PSR J0437–4715, etc. The mean value of this power spectrum is related to the root mean square (rms) random noise σ in the time domain, by the generalized Perseval-Rayleigh theorem for digitized signals (Bracewell (1986)). This σ value was used to normalize the original time series, so that it is now in units of the snr.

How does this snr compare with that obtained by AMDV? A direct comparison is not possible since AMDV mention only the flux density of their spikes and not their snr; they also do not specify the two data files they worked with. However in the caption of their fig. 1 they state that “These spikes are about a third of the height of the largest seen in the whole data set”; since the largest spike in their fig. 1 has a height $\gtrsim 100$ Jansky (Jy), one can assume that the height of their largest spike was $\gtrsim 300$ Jy. Now, the theoretically expected σ for the total power mode of observation at ORT for an 8 MHz (effective) bandwidth and a sampling interval of $102.4\ \mu\text{s}$ is 2.8 Jy, at the best phased condition of ORT; the corresponding number for the phase switched mode of observation is $\sqrt{2}$ times larger (see Vivekanand

(1995)). So the theoretical best snr to be expected by AMDV for their highest spike is $\approx 300/2.8 \approx 107$, which is about twice the number in fig. 1 here. This difference should reduce if one takes into account the noise due to the pulse to pulse flux variations of PSR J0437–4715, reduction in snr due to instrumental effects such as digitization, de-phasing of ORT, etc.

This author feels that it is the σ of this paper that should be operative in estimating the snr of the spikes. However, the later analysis was also repeated with an effective σ that is four times smaller, i.e., with an average snr that is at least two times better than the presumed snr of AMDV, with no change in the essential results.

Next, the positions of the highest 500 spikes in the data file, along with their formal errors, were obtained as discussed in Appendix A. Figure 2 shows the plot of these errors versus the height of the peaks, for data files labelled 50681546 and 50681549; the latter was observed at UT 15:49:39 on 9 Mar 1995 (just 3.35 minutes after the former data file) with the same sampling interval ($102.4\ \mu\text{s}$), and represents yet another file containing very high sensitivity data. The positional errors are inversely correlated with heights, as expected from Appendix A. While the highest peak in both files has a positional error of $\approx 3.5\ \mu\text{s}$, the mean positional error in the two files is $\approx 7.5\ \mu\text{s}$ with standard deviation of $\approx 1.5\ \mu\text{s}$. This is due to the rapidly decreasing number of spikes with increasing spike height.

The positions obtained here are consistent with those of Vivekanand (2000). The main differences are (1) the former are obtained from the original time series data, while the latter were obtained from the re sampled and folded data, and (b) the former are obtained by a weighted mean, while the latter were obtained by fitting Gaussian to the spikes.

Then, the positions of the spikes in each file were obtained modulo the pulsar period. A positive (negative) error in the period used will systematically reduce (increase) the positions of the spikes that arrive later in the data file. This will tend to space out the spikes in the integrated profile, which might give the impression of an **enhanced contrast** of a fringe like distribution of their positions. So the pulsar period was optimized so as to give the narrowest distribution of the positions of the spikes in each data file; this turned out to be $5757.436 \pm 0.001\ \mu\text{s}$, which is consistent with the value of $5757.4365\ \mu\text{s}$ obtained using the prediction mode of the TEMPO timing package. The following results are similar irrespective of which period is used.

Then each of the 500 spikes was replaced by a normalized Gaussian, centered at the estimated position of the spike within the period, having an rms width equal to the estimated positional error. The resulting probability density of occurrence of the position of the spikes is shown in fig. 3 for the two data files mentioned above. The lower panels of fig. 3 show an expanded view of the probability density functions in the central peak of the integrated profile. Clearly there is no evidence for modulation by fringes of any periodicity; a power spectrum analysis of these profiles confirms the conclusion.

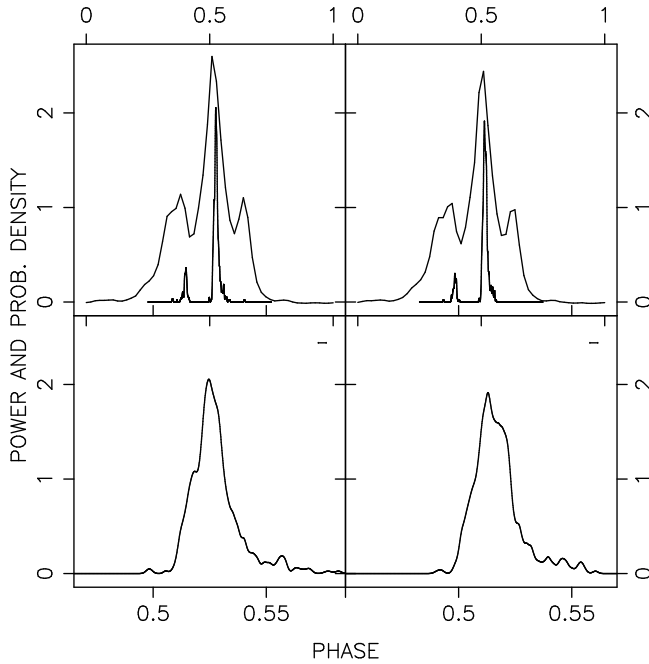


Figure 3. Similar to Fig. 2 of AMDV. **Top panels:** The integrated profiles of data files labelled 50681546 (left) and 50681549 (right). Also shown is the probability density (un-normalized) of the position of the 500 strongest spikes, for each data file. **Bottom panels:** Expanded view of the probability density in the region of the central component of the integrated profiles. The abscissa are in units of the period (5757.4365 μ s), while the ordinates are in arbitrary units. The horizontal bar at the top right corner of the bottom two panels represents a duration of 20 μ s.

3 COMPARISON WITH THE METHOD OF AMDV

The probability density function of the positions of the spikes (fig 3) is the sum of several narrow Gaussian – their widths are much smaller than the range of abscissa that they are spread over. For a limited number of spikes this might naturally give rise to what might appear to be a fringing over the broad distribution. The real issue is whether there is a persistent periodicity in these fringes, which does not vanish as the number of spikes is increased.

3.1 Error estimation

The main difference between AMDV and this work is the estimation of the rms errors on the positions of spikes. AMDV use a uniform value of 1.7 μ s for all 500 spikes in a file, obtained by means of “Monte Carlo analysis”. This work estimates them self-consistently from the data. They range from about 3.2 μ s to 12.3 μ s in the two data files combined, with an average value of about 7.5 μ s in each data file. Therefore AMDV’s errors are on the average 7.5 / 1.7 \approx 4.4 times smaller, and are independent of the snr of the spikes.

Their justification is that “Nyquist reconstruction (Bracewell 1965) allows exact recovery of the underlying band-limited continuous function (pulsar signal plus noise) ...”; and therefore “in these distributions there is almost no noise in the traditional sense”.

While the former statement is correct, the latter is not. Nyquist reconstruction will not separate the signal from the noise; it will reconstruct only their sum. So the estimation of any parameter of the signal (say, the position of a spike) will involve uncertainty due to the noise; the estimation error on such a parameter must depend upon the actual snr of the signal buried in the noise. Stronger spikes should have their positions estimated more accurately; Appendix A shows a simple method of estimating this accuracy.

Another way of looking at this problem is the following. To obtain arbitrarily small errors on the positions of the spikes, one needs arbitrarily large number of ordinates, of a given snr. Now, it is true that by Nyquist reconstruction one can synthesize an infinite (in principle) number of ordinate values in any given abscissa range; and each one of them will have the same rms error as of the original data (Bracewell (1986)). However, not all of the synthesized ordinates will have **independent** noise; only those separated by the sampling interval will. So the errors on the positions of the spikes can not be very different from that derived in Appendix A.

This author can think of no way he could have overestimated the **average** positional errors of the spikes by a factor of 4.4.

On the other hand, is there a possibility of **underestimating** the positional errors of spikes? The model assumed in Appendix A is that of additive (system) noise. If one assumes that the pulsar signal is also noise like, for example an amplitude modulated noise (AMN) according to Rickett (1975), one would have to add this so called **self noise** (Goodman (1985), Vivekanand & Kulkarni (1991)) to the system noise. However, the σ of section 2 includes all forms of noise present in the data, since it has been estimated from the data itself, so the AMN model is unlikely to change the results of this work. Even then, the AMN model of the pulsar signal may make it harder for AMDV to justify their positional errors.

3.2 Averaging two probability distributions

Another difference is that AMDV do not average coherently the two (presumed fringing) probability distributions of their fig. 2 (similar to fig. 3 here). If indeed there is a coherent periodicity in the two data files, their average power spectrum must enhance (or at least not reduce) the contrast of this spectral feature, unless the periodicity is changing from file to file.

Figure 4 shows the probability density functions of the position of the spikes in the two data files, along with the corresponding power spectrum (the probability distribution of the second file has been shifted by the appropriate amount to align with the first, using a cross-correlation). In this figure all positional errors have been set to a constant 1.7 μ s, to recreate (if possible) the results of AMDV. There appears to be no real harmonic relation between the spectral features in each of the top two panels of fig. 4. Moreover the spectra of the two files are not similar. This is disturbing, since the duration of each file is \approx 1.16 minutes, and they are separated in observing time by only 3.35 minutes; a spectral feature that can change significantly in the latter time is unlikely to be considered stable in the former time, except by a special design. The bottom panel of fig. 4 shows the average of

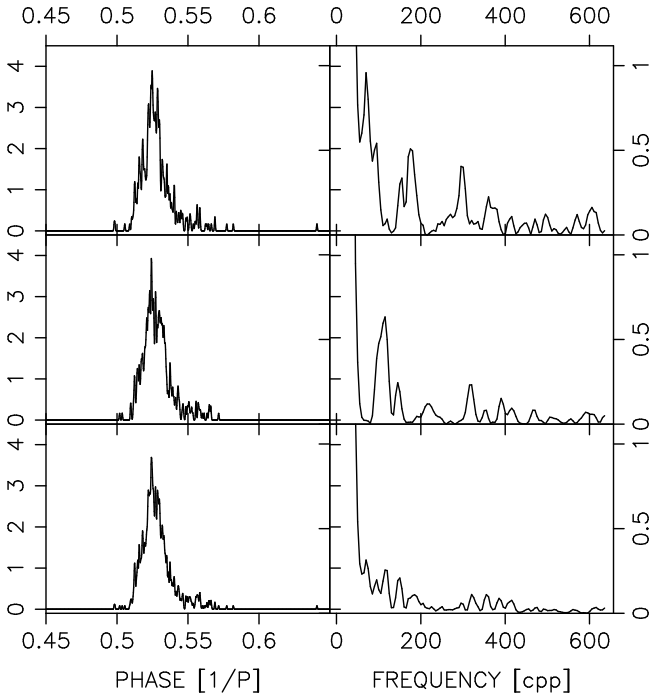


Figure 4. Left Panels: Probability density (un-normalized) of the position of the 500 strongest spikes in a data file, using a fixed error of $1.7 \mu\text{s}$ for all positions; this is equal to the FWHM of $4.0 \mu\text{s}$ used by AMDV. Only the distribution in the central component of the integrated profile is considered. The abscissae are in units of the period ($5757.4365 \mu\text{s}$), while the ordinates are in arbitrary units. **Right Panels:** The corresponding power spectrum; the abscissae are in units of cycles per period (cpp), while the ordinates are in arbitrary units. **Top pair** of figures refer to data file 50681546 while the **middle pair** refer to data file 50681549; the probability density of the latter has been shifted so as to be aligned to that of the former. The **bottom pair** refer to the average of the two data files.

the top two probability distributions, and the corresponding power spectrum. The relative power in any spectral feature has only reduced. This remains true even for the average of the two power spectra (top right and middle right panels).

If at all there is a fundamental periodicity in the data, it is more likely to be at ≈ 175 (cpp), which is equal to a periodicity of $\approx 33 \mu\text{s}$, and not at $\approx 20 \mu\text{s}$ obtained by AMDV. From the width of this feature as well as the widths of its **presumed** harmonics, one is unlikely to see “nine fairly evenly spaced sub peaks” in the probability function as claimed by AMDV; if at all, three or four sub peaks are expected to be seen. However, this is not the case actually. Some low frequencies were filtered from the average (complex) spectrum and an inverse Fourier transform was done to bring out the quasi periodicities in the data, if any; nothing similar to that seen by AMDV, or similar to that discussed above, was observed.

Similar results were obtained when the period used in fig. 4 was the optimized value of $5757.436 \mu\text{s}$.

Figure 4 was also obtained with two modifications – using positional errors that were (a) half and (b) quarter of the original values for each spike, respectively. The corresponding probability density of occurrence of the position of the spikes becomes less smooth as compared to the bot-

tom panels of fig. 3, and similar to the left top two panel of fig. 4, but does not show any fringing. This is equivalent to increasing the effective signal to noise ratio of the data by factors 2 and 4, respectively. In other words, even if this work has made an error of a factor of 4 in **labelling** the snr values of the individual samples (the relative snr values do not change), the results are essentially the same.

3.3 Choice of period

Yet another possibility is the choice of a wrong effective period by AMDV. They state that they used a period given by “a computed ephemeris with recent timing parameters”; but they neither quote the value used nor mention that they optimized it as discussed above. The header in the two data files contains the value $5757.4409 \mu\text{s}$; this is computed by the online software for online folding of pulsar data, and is expected to be very accurate. In case AMDV have used this value of the period, they would have made an error of 4.4 nano seconds. This would lead to a systematic shift of approximately $12\,000 \text{ periods} \times 0.0044 \mu\text{s} \approx 53 \mu\text{s}$ between the first and last spike in the data file. Now spreading out of very narrow peaks along the abscissa can lead to voids in their distribution, and can simulate “fringes” in their position distribution.

4 ACKNOWLEDGEMENT

I thank the referee for suggesting the AMN model, and an important clarification regarding the period used in this paper.

REFERENCES

Ables, J. G., McConnell, D., Deshpande, A. A., Vivekanand, M., 1997, *ApJ*, 475, L33
 Bracewell, R. N., 1986, *The Fourier Transform and its Applications*, McGraw-Hill, New York.
 Goodman, J. W., 1985, *Statistical Optics*, (New York: Wiley Interscience)
 Jenet, F. A., Anderson, S. B., Kaspi, V. M., Prince, T. A., Unwin, S. C., 1998, *ApJ*, 498, 365
 Rickett, B. J., 1975, *ApJ*, 197, 185
 Vivekanand, M., 1995, *MNRAS*, 274, 785
 Vivekanand, M., 2000, *ApJ*, 543, 979
 Vivekanand, M., Ables, J. G., McConnell, D., 1998, *ApJ*, 501, 823
 Vivekanand, M., Kulkarni, S. R., 1991, *Radio interferometry: Theory, techniques, and applications*, Proceedings of the 131st IAU Colloquium, San Francisco, Astronomical Society of the Pacific, 1991, pp. 1-5

APPENDIX A: POSITIONS AND ERRORS OF SPIKES

Let the abscissa and the ordinate in the bottom panel of fig. 1 be labelled x and y , respectively. After trial and error, it was found that $N = 5$ time samples adequately represent a typical spike, for the purpose of estimating its position and the error on the position. The mean position was obtained by the weighted average

$$\phi = \frac{\sum_{i=1}^N x_i \times y_i}{\sum_{j=1}^N y_j}; \Rightarrow \langle \phi \rangle \approx \frac{\sum_{i=1}^N x_i \times y_{0i}}{\sum_{j=1}^N y_{0j}}, \quad (A1)$$

the third sample being at the peak of the spike; y_{0i} is the true pulsar flux (in units of snr) while $dy_i = y_i - y_{0i}$ is the small variation due to random noise of variance 1.0 (by definition). Then the deviation $d\phi$ is given by

$$\begin{aligned} d\phi &= \frac{\sum_{i=1}^N x_i \times dy_i}{\sum_{j=1}^N y_{0j}} - \frac{[\sum_{i=1}^N x_i \times y_{0i}] \times [\sum_{j=1}^N dy_j]}{\left[\sum_{k=1}^N y_{0k}\right]^2} \\ &\approx \frac{\sum_{i=1}^N (x_i - \langle \phi \rangle) \times dy_i}{\sum_{j=1}^N y_{0j}}. \end{aligned} \quad (A2)$$

Therefore the variance in the position σ_ϕ^2 is given by

$$\sigma_\phi^2 = \langle d\phi^2 \rangle = \frac{N \times \sigma_x^2}{\left[\sum_{i=1}^N y_{0i}\right]^2}; \Rightarrow \sigma_\phi = \frac{\sqrt{N} \times \sigma_x}{\sum_{i=1}^N y_{0i}}, \quad (A3)$$

where σ_x is the standard deviation of the abscissa range used.

For a fixed N , and therefore a fixed denominator in eq. A3, the error on the position σ_ϕ varies linearly with the range of abscissa used (σ_x), as is expected. For a fixed range of abscissa, the denominator varies as N , so that σ_ϕ varies inversely as \sqrt{N} ; this is also expected, provided each of the N values of the ordinate are independent measurements. The σ_ϕ is inversely proportional to the average signal to noise ratio of the data.

To obtain an idea of the positional errors to be expected, let $N = 5$. For a uniform range of 5 time samples of duration 102.4 μ s each, $\sigma_x = 5.0 \times 102.4/\sqrt{12} \approx 147.8 \mu$ s. The sum of the five ordinates around the spike is 92.8 in the bottom panel of fig 1. Therefore $\sigma_\phi = \sqrt{5} \times 147.8/92.8 \approx 3.6 \mu$ s. This is the best positional error in the current data, since this is the highest peak analyzed.